Core–Shell Nanostructures

Deutsche Ausgabe: DOI: 10.1002/ange.201506157
Internationale Ausgabe: DOI: 10.1002/anie.201506157

Establishing the Structural Integrity of Core–Shell Nanoparticles against Elemental Migration using Luminescent Lanthanide Probes

*Bing Chen, Dengfeng Peng, Xian Chen, Xvsheng Qiao, Xianping Fan, and Feng Wang**

Abstract: *Core–shell structured nanoparticles are increasingly used to host luminescent lanthanide ions but the structural integrity of these nanoparticles still lacks sufficient understanding. Herein, we present a new approach to detect the diffusion of dopant ions in core–shell nanostructures using luminescent lanthanide probes whose emission profile and luminescence lifetime are sensitive to the chemical environment. We show that dopant ions in solution-synthesized core–shell nanoparticles are firmly confined in the designed locations. However, annealing at certain temperatures (greater than circa 350°C) promotes diffusion of the dopant ions and leads to degradation of the integrity of the nanoparticles. These insights into core–shell nanostructures should enhance our ability to understand and use lanthanide-doped luminescent nanoparticles.*

Over the last ten years, there has been an increasing focus on the synthesis of lanthanide-doped nanoparticles for applications in biological imaging, photonics, photovoltaics, and therapeutics.[1–4] Given the limited scope to design homogeneously doped nanoparticles with particular optical properties, core–shell structural engineering has emerged as a powerful means to construct novel lanthanide-doped nanoparticles by integrating functionalities and regulating the complex interplay of lanthanide interactions.[5] However, although current synthetic approaches allow for controlled incorporation of various lanthanide ions into separate layers of a core–shell nanoparticle, it remains unknown whether the structural integrity of the nanostructure is maintained against elemental migration across the core–shell interface. Conventionally, core–shell structures are investigated by electron microscopy in combination with high-angle annular dark field imaging (HAADF), electron energy loss spectroscopy (EELS), and energy-dispersive X-ray spectroscopy (EDS), techniques which typically lack the sensitivity to detect trace amount of dopant ions.[6]

[*] B. Chen, Dr. D. Peng, X. Chen, Prof. F. Wang
Department of Physics and Materials Science
City University of Hong Kong
83 Tat Chee Avenue, Hong Kong SAR (China)
E-mail: fwang24@cityu.edu.hk
B. Chen, Prof. X. Qiao, Prof. X. Fan
State Key Laboratory of Silicon Materials
School of Materials Science and Engineering
Zhejiang University, Hangzhou 310027 (China)
Prof. F. Wang
City University of Hong Kong Shenzhen Research Institute
Shenzhen 518057 (China)

Supporting information for this article is available on the WWW under http://dx.doi.org/10.1002/anie.201506157.

Herein, we present a new approach to investigate the integrity of core–shell nanostructures by using Tb^{3+} and Ce^{3+} dopant ions as luminescent probes. As shown in Figure 1, when a Ce^{3+}-doped nanoparticle core is co-doped with Tb^{3+}, Ce^{3+} will have a shorter decay lifetime as a result of energy transfer from Ce^{3+} to Tb^{3+} (Figure 1a and b).[7] Although the time decay of the Ce^{3+} ion is not sensitive to low concentrations of Tb^{3+} (for example less than 0.5 mol%), sharp emission bands for Tb^{3+} ions appear at $\lambda = 381$ nm, 416 nm, and 437 nm (Figure 1c), owing to suppressed $^5D_3 + {}^7F_6 \rightarrow {}^5D_4 + {}^7F_0$ cross-relaxations at large Tb···Tb interatomic separations (Figure 1d).[8] Notably, these emission bands can be clearly detected even when only a trace amount of Tb^{3+} is present (such as 0.1 mol%), thus serving as unambiguous evidence for the presence of Tb^{3+} ions. Therefore, the spectral characteristics of Ce^{3+} and Tb^{3+} ions together provide a sensitive probe of the chemical composition of the host lattice.

As a proof-of-concept experiment to probe the actual location of dopant ions in the core–shell nanostructured hosts,

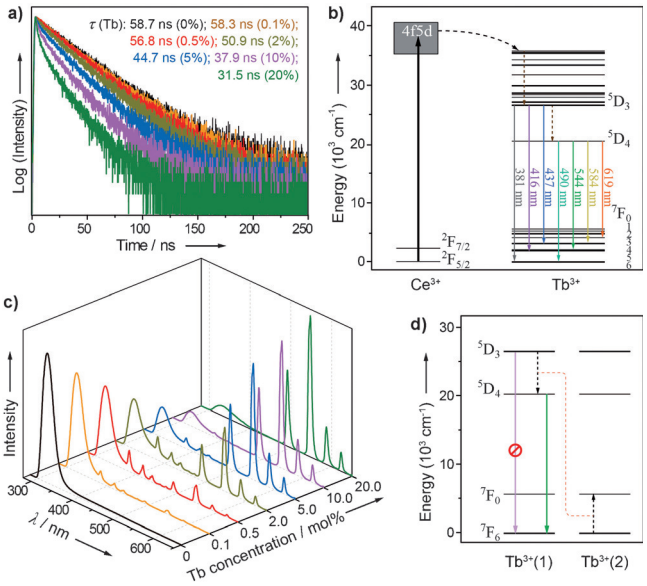

Figure 1. a) Luminescence decay curves of Ce^{3+} in $NaYF_4$:Ce/Tb@$NaYF_4$ core–shell nanoparticles ($[Ce^{3+}] = 20$ mol%; $[Tb^{3+}] = 0$–20 mol%). In this case, the $NaYF_4$ shell protects the core layer from surface quenching. b) Simplified energy-level structures showing non-radiative energy transfer from Ce^{3+} to Tb^{3+}. c) Emission spectra of $NaYF_4$:Ce/Tb@$NaYF_4$ nanoparticles ($[Ce^{3+}] = 20$ mol%; $[Tb^{3+}] = 0$–20 mol%). d) Simplified energy-level diagram showing cross-relaxation between Tb^{3+} ions. Note that emission from the high-lying $^5D_3$ excited state can be completely quenched at high Tb^{3+} concentrations (such as at 20 mol%). Luminescence decay curves and emission spectra were all recorded with an excitation wavelength of $\lambda_{exc} = 264$ nm.

we fabricated a $NaYF_4$@$NaYF_4$ nanoparticle doped with Ce^{3+} (20 mol%) and Tb^{3+} ions (20 mol%) in the core and shell layers, respectively. As designed, the Ce^{3+} and Tb^{3+} ions are spatially separated to eliminate mutual interactions. Furthermore, the configuration also quenches $^5D_3$ emissions of Tb^{3+} because of a high Tb^{3+} concentration.

The nanoparticles were synthesized through a widely used layer-by-layer coating process carried out in organic solutions,[9] which involves the growth of a $NaYF_4$:Ce core nanoparticle followed by the epitaxial deposition of a $NaYF_4$:Tb shell (see the Supporting Information). Transmission electron microscopy (TEM) micrographs reveal a quasi-spherical shape of the as-synthesized core–shell nanoparticle (Figure 2a). EELS analysis shows that the

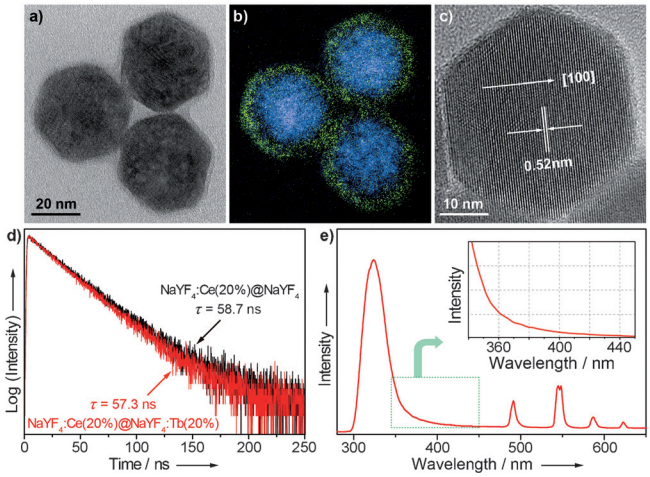

Figure 2. a) Typical TEM image of the as-synthesized $NaYF_4$:Ce@$NaYF_4$:Tb core–shell nanoparticles. b) Element maps of Ce (blue) and Tb (green) in the nanoparticles shown in (a). c) High-resolution TEM image of a nanoparticle shows that it is single crystalline in nature and has a *d* spacing of 0.52 nm in the crystalline plane. d) Decay curves of Ce^{3+} in the as-synthesized $NaYF_4$:Ce@$NaYF_4$:Tb and $NaYF_4$:Ce@$NaYF_4$ nanoparticles, respectively. e) Emission spectrum of the as-synthesized $NaYF_4$:Ce@$NaYF_4$:Tb nanoparticles. The dopant concentrations of Ce^{3+} and Tb^{3+} are both 20 mol%. Luminescence decay curves and the emission spectrum were all recorded with λ_{exc} = 264 nm.

distributions of Ce^{3+} and Tb^{3+} elements in the nanoparticles are very consistent with the designed compositions (Figure 2b), confirming the core–shell structure of the nanoparticles. High-resolution TEM image (Figure 2c) reveals a single-crystalline structure for the core–shell nanoparticle and lattice fringes with a measured *d* spacing of 0.52 nm, which is in good agreement with the lattice spacing in the (100) planes of hexagonal phase $NaYF_4$ (0.515 nm; Joint Committee on Powder Diffraction Standards file number 16-0334).

We next probed the fine structure of the core–shell nanoparticles by combining time-resolved and steady-state luminescence of Ce^{3+} and Tb^{3+} ions. As shown in Figure 2d, we detected only a marginal decrease in the lifetime of Ce^{3+} in the $NaYF_4$:Ce@$NaYF_4$:Tb core–shell nanoparticles with respect to that in the control sample which had Tb^{3+}-free shell (57.3 versus 58.7 ns). The comparison reveals a very limited interaction between Ce^{3+} and Tb^{3+} ions in the core–shell structure. However, we only detected emission bands originating from the $^5D_4$ state of Tb^{3+} in the steady-state emission spectra (Figure 2e), implying no leakage of Tb^{3+} ions from the shell layer. Otherwise, a region of low Tb^{3+} concentration would be created in the core lattice and give rise to $^5D_3$ emission bands. Taken together, we can conclude that the Ce^{3+}–Tb^{3+} interaction primarily occurred at the core–shell interface leading to the weak detected $^5D_4$ emission bands of Tb^{3+}, thereby corroborating the firm confinement of Ce^{3+} and Tb^{3+} dopants in the core and shell layers, respectively.

The high degree of structural integrity is attributed to the substitutional nature of the dopant ions in the host lattice as well as the close-packed lattice structure. Owing to their large ionic sizes, lanthanide dopant ions are unlikely to migrate in the host lattice without the assistance of vacancies. At relatively low temperatures (such as, for example, at the synthesis temperature of 290°C), the diffusion of dopant ions is sluggish because of the insufficient vibrational energy of the atoms and a lack of vacant sites. As both thermal excitation of atoms and the concentration of vacancies grow rapidly with increasing temperature,[10] the migration of dopant ions may be activated at elevated temperatures and may induce damage to the core–shell nanostructures.

To evaluate the thermal stability of the core–shell structure, we annealed the as-synthesized nanoparticles at varying temperatures (350–450°C). TEM characterization (Figure 3a–c) and EELS analysis (see Figure S1 in the Supporting Information) show that the particle size, morphology, and the layered structure are essentially preserved

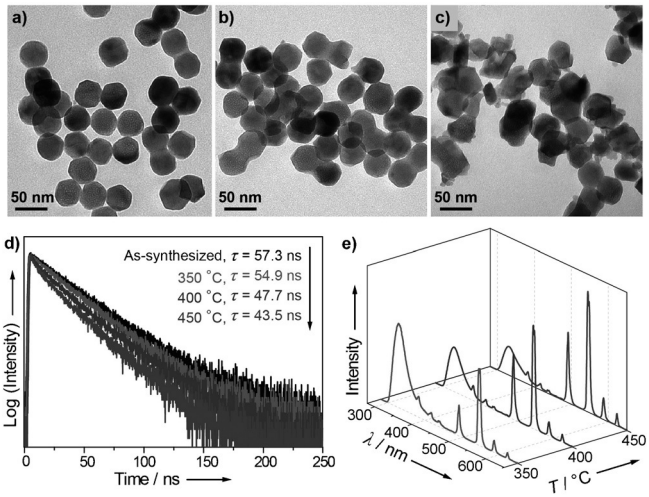

Figure 3. a–c) TEM images of the $NaYF_4$:Ce@$NaYF_4$:Tb core–shell nanoparticles after annealing for 120 min at 350°C, 400°C, and 450°C, respectively. d) Luminescence decay curves of Ce^{3+} ions in the $NaYF_4$:Ce@$NaYF_4$:Tb ([Ce^{3+}] = 20 mol%; [Tb^{3+}] = 20 mol%) core–shell nanoparticles before and after annealing, respectively. e) Emission spectra of the $NaYF_4$:Ce@$NaYF_4$:Tb ([Ce^{3+}] = 20 mol%; [Tb^{3+}] = 20 mol%) core–shell nanoparticles after annealing. Luminescence decay curves and emission spectra were all recorded with λ_{exc} = 264 nm.

after annealing. X-ray powder diffraction (XRD) patterns (Figure S2) further confirm that the phase of the annealed samples is consistent with that of the corresponding as-synthesized sample. Therefore, substantial recrystallization and growth of the crystalline grains are excluded. However, we detected an appreciable decrease in the Ce^{3+} lifetime with increasing annealing temperature (Figure 3d), indicating a relocation of dopant ions within the nanoparticles. The migration of dopant ions across the core–shell interface is further validated by the presence of a $^5D_3$ emission band for Tb^{3+} ions in the annealed samples (Figure 3e).

In conclusion, a new approach has been developed and validated to investigate the integrity of core–shell nanostructures. Spectroscopic investigations of the as-synthesized core–shell nanoparticles indicate that the dopant ions are firmly confined in their designed locations. However, heat treatment at elevated temperatures (above circa 350 °C) promotes migration of dopant ions and degrades the structural integrity. Our study will substantially improve our understanding of nanostructured materials comprising lanthanide dopants, in addition to providing a general guideline for the proper use of these nanomaterials in technological applications.

Acknowledgements

This work was supported by the Research Grants Council of Hong Kong (CityU 109413) and the National Natural Science Foundation of China (Nos. 21303149 and 51332008).

Keywords: core–shell nanoparticles · electron microscopy · energy transfer · lanthanides · photophysics

How to cite: *Angew. Chem. Int. Ed.* **2015**, *54*, 12788–12790
Angew. Chem. **2015**, *127*, 12979–12981

[1] a) S. K. Maji, S. Sreejith, J. Joseph, M. Lin, T. He, Y. Tong, H. Sun, S. W. K. Yu, Y. Zhao, *Adv. Mater.* **2014**, *26*, 5633; b) S. H. Nam, Y. M. Bae, Y. I. Park, J. H. Kim, H. M. Kim, J. S. Choi, K. T. Lee, T. Hyeon, Y. D. Suh, *Angew. Chem. Int. Ed.* **2011**, *50*, 6093; *Angew. Chem.* **2011**, *123*, 6217; c) C. Wang, L. Cheng, H. Xu, Z. Liu, *Biomaterials* **2012**, *33*, 4872; d) B. Liu, Y. Chen, C. Li, F. He, Z. Hou, S. Huang, H. Zhu, X. Chen, J. Lin, *Adv. Funct. Mater.* **2015**, *25*, 4717; e) M. Wang, C.-C. Mi, W.-X. Wang, C.-H. Liu, Y.-F. Wu, Z.-R. Xu, C.-B. Mao, S.-K. Xu, *ACS Nano* **2009**, *3*, 1580; f) H. Xing, W. Bu, S. Zhang, X. Zheng, M. Li, F. Chen, Q. He, L. Zhou, W. Peng, Y. Hua, *Biomaterials* **2012**, *33*, 1079; g) Y. Sun, X. Zhu, J. Peng, F. Li, *ACS Nano* **2013**, *7*, 11290.

[2] a) D. Peng, Q. Ju, X. Chen, R. Ma, B. Chen, G. Bai, J. Hao, X. Qiao, X. Fan, F. Wang, *Chem. Mater.* **2015**, *27*, 3115; b) H. Zhu, X. Chen, L. M. Jin, Q. J. Wang, F. Wang, S. F. Yu, *ACS Nano* **2013**, *7*, 11420; c) B. Voss, M. Haase, *ACS Nano* **2013**, *7*, 11242; d) A. D. Ostrowski, E. M. Chan, D. J. Gargas, E. M. Katz, G. Han, P. J. Schuck, D. J. Milliron, B. E. Cohen, *ACS Nano* **2012**, *6*, 2686; e) Y. Zhou, S.-T. Han, X. Chen, F. Wang, Y.-B. Tang, V. Roy, *Nat. Commun.* **2014**, *5*, 4720; f) R. Deng, F. Qin, R. Chen, W. Huang, M. Hong, X. Liu, *Nat. Nanotechnol.* **2015**, *10*, 237; g) M. Quintanilla, F. Ren, D. Ma, F. Vetrone, *ACS Photonics* **2014**, *1*, 662.

[3] a) R. Naccache, F. Vetrone, J. A. Capobianco, *ChemSusChem* **2013**, *6*, 1308; b) H. Q. Wang, M. Batentschuk, A. Osvet, L. Pinna, C. J. Brabec, *Adv. Mater.* **2011**, *23*, 2675; c) H. Lian, Z. Hou, M. Shang, D. Geng, Y. Zhang, J. Lin, *Energy* **2013**, *57*, 270; d) L. Liang, Y. Liu, X.-Z. Zhao, *Chem. Commun.* **2013**, *49*, 3958; e) G. B. Shan, G. P. Demopoulos, *Adv. Mater.* **2010**, *22*, 4373.

[4] a) N. M. Idris, M. K. Gnanasammandhan, J. Zhang, P. C. Ho, R. Mahendran, Y. Zhang, *Nat. Med.* **2012**, *18*, 1580; b) G. Tian, Z. Gu, L. Zhou, W. Yin, X. Liu, L. Yan, S. Jin, W. Ren, G. Xing, S. Li, *Adv. Mater.* **2012**, *24*, 1226; c) D. Yang, X. Kang, Y. Dai, Z. Hou, Z. Cheng, C. Li, J. Lin, *Biomaterials* **2013**, *34*, 1601; d) G. Wang, Q. Peng, Y. Li, *Acc. Chem. Res.* **2011**, *44*, 322; e) Y.-F. Wang, G.-Y. Liu, L.-D. Sun, J.-W. Xiao, J.-C. Zhou, C.-H. Yan, *ACS Nano* **2013**, *7*, 7200; f) P. Huang, W. Zheng, S. Zhou, D. Tu, Z. Chen, H. Zhu, R. Li, E. Ma, M. Huang, X. Chen, *Angew. Chem. Int. Ed.* **2014**, *53*, 1252; *Angew. Chem.* **2014**, *126*, 1276.

[5] a) H. Wen, H. Zhu, X. Chen, T. F. Hung, B. Wang, G. Zhu, S. F. Yu, F. Wang, *Angew. Chem. Int. Ed.* **2013**, *52*, 13419; *Angew. Chem.* **2013**, *125*, 13661; b) Z. Li, Y. Zhang, S. Jiang, *Adv. Mater.* **2008**, *20*, 4765; c) F. Vetrone, R. Naccache, V. Mahalingam, C. G. Morgan, J. A. Capobianco, *Adv. Funct. Mater.* **2009**, *19*, 2924; d) G. Chen, H. Ågren, T. Y. Ohulchanskyy, P. N. Prasad, *Chem. Soc. Rev.* **2015**, *44*, 1680; e) R. Ghosh Chaudhuri, S. Paria, *Chem. Rev.* **2012**, *112*, 2373; f) C. Dong, A. Korinek, B. Blasiak, B. Tomanek, F. C. van Veggel, *Chem. Mater.* **2012**, *24*, 1297; g) M.-K. Tsang, G. Bai, J. Hao, *Chem. Soc. Rev.* **2015**, *44*, 1585; h) Y. Liu, D. Wang, L. Li, Q. Peng, Y. Li, *Inorg. Chem.* **2014**, *53*, 3257; i) C. Zhang, J. Y. Lee, *ACS Nano* **2013**, *7*, 4393; j) H. Schäfer, P. Ptacek, O. Zerzouf, M. Haase, *Adv. Funct. Mater.* **2008**, *18*, 2913.

[6] a) L. Wang, H. Dong, Y. Li, R. Liu, Y. F. Wang, H. K. Bisoyi, L. D. Sun, C. H. Yan, Q. Li, *Adv. Mater.* **2015**, *27*, 2065; b) F. Zhang, R. Che, X. Li, C. Yao, J. Yang, D. Shen, P. Hu, W. Li, D. Zhao, *Nano Lett.* **2012**, *12*, 2852; c) D. Chen, P. Huang, *Dalton Trans.* **2014**, *43*, 11299; d) J. Liu, Y. Liu, W. Bu, J. Bu, Y. Sun, J. Du, J. Shi, *J. Am. Chem. Soc.* **2014**, *136*, 9701; e) N. J. Johnson, F. C. van Veggel, *Nano Res.* **2013**, *6*, 547; f) N. J. Johnson, A. Korinek, C. Dong, F. C. van Veggel, *J. Am. Chem. Soc.* **2012**, *134*, 11068; g) X. Li, F. Zhang, D. Zhao, *Chem. Soc. Rev.* **2015**, *44*, 1346; h) W. Feng, C. Han, F. Li, *Adv. Mater.* **2013**, *25*, 5287; i) See Ref. [5i]; j) X. Liu, R. Deng, Y. Zhang, Y. Wang, H. Chang, L. Huang, X. Liu, *Chem. Soc. Rev.* **2015**, *44*, 1479; k) H. Schäfer, P. Ptacek, K. Hickmann, M. Prinz, M. Neumann, M. Haase, *Russ. J. Inorg. Chem.* **2009**, *54*, 1914.

[7] a) H. Kiliaan, J. Kotte, G. Blasse, *J. Electrochem. Soc.* **1987**, *134*, 2359; b) K. Riwotzki, H. Meyssamy, H. Schnablegger, A. Kornowski, M. Haase, *Angew. Chem. Int. Ed.* **2001**, *40*, 573; *Angew. Chem.* **2001**, *113*, 574; c) G. Bühler, C. Feldmann, *Angew. Chem. Int. Ed.* **2006**, *45*, 4864; *Angew. Chem.* **2006**, *118*, 4982; d) V. Pankratov, A. Popov, S. Chernov, A. Zharkouskaya, C. Feldmann, *Phys. Status Solidi B* **2010**, *247*, 2252.

[8] a) D. Robbins, B. Cockayne, B. Lent, J. Glasper, *Solid State Commun.* **1976**, *20*, 673; b) C.-K. Duan, C.-C. Ko, G. Jia, X. Chen, P. A. Tanner, *Chem. Phys. Lett.* **2011**, *506*, 179; c) Q. Su, S. Han, X. Xie, H. Zhu, H. Chen, C.-K. Chen, R.-S. Liu, X. Chen, F. Wang, X. Liu, *J. Am. Chem. Soc.* **2012**, *134*, 20849; d) B. Chen, X. Qiao, D. Peng, X. Fan, *J. Phys. Chem. C* **2014**, *118*, 30197.

[9] a) F. Wang, R. Deng, X. Liu, *Nat. Protoc.* **2014**, *9*, 1634; b) X. Chen, D. Peng, Q. Ju, F. Wang, *Chem. Soc. Rev.* **2015**, *44*, 1318.

[10] D. A. Porter, K. E. Easterling, M. Sherif, *Phase Transformations in Metals and Alloys*, 3nd ed., CRC Press, Boca Raton, FL, **2009**.

Received: July 4, 2015
Published online: August 28, 2015

